International Journal of Communication Networks and Information Security

ISSN: 2073-607X, 2076-0930

*Volume **14** Issue **02 Year 2022** Page **66:82***

Performance Exploration of Uncertain RF MEMS Switch Design with Uniform Meanders

C Leela Mohan[1], **K Ch Sri Kavya**[2], **K Sarat Kumar**[3]

[1]*Research Scholar, Dept. of ECE, KL Deemed to be University, Andhra Pradesh, India*

[2, 3] *Professor, Dept. of ECE, KL Deemed to be University, Andhra Pradesh, India*

[2]*srinivasgphd@gmail.com*

Article History

Received: 18 Feb 2022
Revised: 30 May 2022
Accepted: 16 June 2022

Abstract

The design of RF-MEMS Switch is useful for future artificial intelligence applications. Radio detection and range estimation has been employed with RF MEMS technology. Attenuators, limiters, phase shifters, T/R switches, and adjustable matching networks are components of RF MEMS. The proposed RF MEMS technology has been introduced in T/R modules, lenses, reflect arrays, sub arrays and switching beam formers. The uncertain RF MEMS switches have been faced many issues like switching and voltage alterations. This study aims in the direction of design, simulation, model along with RF MEMS switching analysis including consistent curving or meandering. The proposed RF MEMS Switch is a flexure form of the Meanders that attain minimal power in nominal voltage. Moreover, this research work highlights the materials assortment in case of beam along with signal-based dielectric. The performance analysis is demonstrated for various materials that have been utilized in the design purpose. Further, better isolation is accomplished at the range of -31dB necessary regarding 8.06V pull-in voltage through a spring constant valued at 3.588N/m, switching capacitance analysis has been found to be 103 fF at ON state and 7.03pF at OFF state and the proposed switch is optimized to work at 38GHz. The designed RF MEMS switch is giving 30% voltage improvement; switching frequency is improved by 21.32% had been attained, which are outperformance the methodology and compete with present technology.

Keywords: COMSOL, HFSS, uncertain-RF-MEMS-Switch, Meanders

1. Introduction

This section, facilitates a brief description about the Micro Electro Mechanical Systems (MEMS) & their application performances, and which is a key changer in today's technology. Most of the IoT (Internet of Things) revolutions, are predicted to increase the link between electronic devices and real-world smart living things. People have been boosting machine to machine communications will be driven by these technologies (M2M). Technology that uses RF MEMS is utilized to detect and switching the activity easily. Switching components including like attenuators, phase shifters, and adjustable matching networks are available in RF MEMS. T/R modules, lenses, and reflector arrays,

as well as sub-array switches may all benefit from the usage of MEMS technology. As a result, microelectromechanical systems (MEMS) are being used in a wide range of fields, including consumer electronics, vehicle safety, autonomous driving, avionics, smart grids, and healthcare facilities. Figure 1 depicts the various applications of MEMS and their importance.

High-frequency MEMS resonators are microelectromechanical structures (MEMS). They are essential components in several of the above-mentioned implementations, including a selection of frequency, timing, inertial detection, optical signals manipulation, energy harvesting, mass/chemical sensing, and mass/chemical sensing, and are used extensively in all of these applications. Extruded planar geometries with a predetermined thickness are used to make MEMS resonators, which are often imprinted in silicon. Because of this, the structure has a primarily 2D layout, yet it generally shows meaningful 3D dynamics. Micromechanical structures are often excited by translating an electrical signal into a force that may be utilized to excite the device in conventional applications. Various capacitive, piezoelectric, thermal, or piezoresistive transduction methods are used to pick up the structure's vibrations and turn them back into an electrical signal.

Miniaturization is the main advantage of MEMS technology. They provide good electrical performance and low consumption [1-4]. These are used for high-frequency applications and are commonly configured with a shunt configuration. In low-frequency applications, they are used with a fixed-wire configuration [6-9]. However, the capability is gained with the capacitive contact switches towards the processing and controlling of high-voltage power. Good isolation is also expected for the switch activation state.

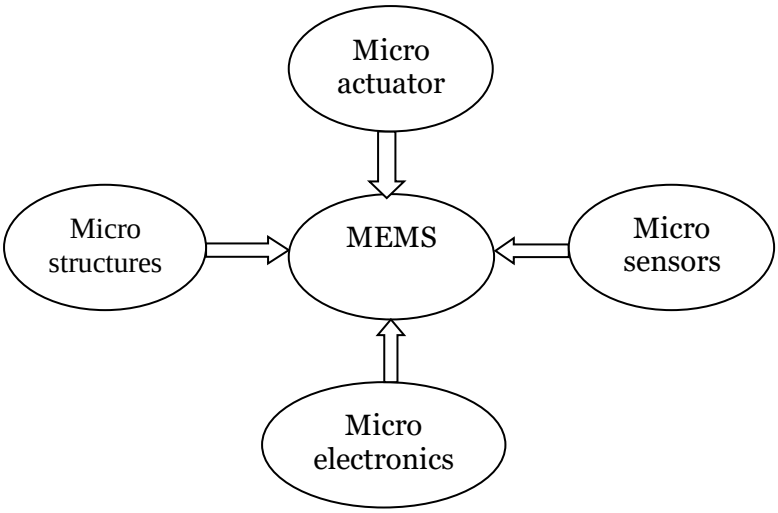

Figure 1 General MEMS applications

As with other MEMS systems, the needed mechanical qualities are often obtained by combining the mechanical properties of preset basic components, such as masses and flexural or torsion springs produced by simple or foldable beam structures. Mechanical components are often adjusted by hand by the design engineer in order to meet the application's specifications, which is a time-consuming and error-prone process. Therefore, the design process is significantly more time-consuming and costly, and it is also dependent on the knowledge of the design engineer Recent market advancements are driving MEMS devices. Shrinkage and power consumption reduction, making device design more critical and structural optimization-based automated design techniques essential for industrial growth. To put it simply, the amount of design flexibility provided by structural optimization approaches may be divided into two groups.

A better design approach for optimizing a switch's functional behavior is achieved by optimizing its isolation and low pull-in voltage. This process is carried out through a proposed method. The proposed design involves introducing meanders in the proposed structure to improve its stability [11]. The design of the switch is based on the various device specifications and the non-uniform meanders. The various components are studied for their mechanical and electromechanical properties [12-14]. With diminished pull in the voltage quantified overlapping area will result in an increment in pull in the current value. In addition, impedance matching is obtained using a high-frequency Ka-band switch [15-16].

The work begins with the introductory part under the proposed methodology that includes the RF MEMS Switch. Later sections deal with the theoretical framework describing various aspects of the proposed Switch and its various components in section 2.

2. Resources and Approaches

In this section, facilitates a brief description about the proposed switch deal with the theoretical framework describing various aspects and its various components. MEMS gyroscopes may benefit from a topology optimization approach for MEMS resonators that was recently published. Single mass resonator suspension structures were restricted to 2D in-plane dynamics and technique development was the primary goal. An academic benchmark example served as a testbed for the paper's optimization proposals, which were subsequently applied to a real-world design problem.
The goal of this study is to apply the topology optimization method described for the structure of MEMS resonators that are useful to industry. Consequently, the thermodynamics of planar structures using suspended proof masses or plates are explored here. This technology may be useful for gyroscope applications that need precise control over the initial eigenfrequencies of both single- and double-mass tuning fork MEMS resonators. In this proposal implementing a lower-order models and Mindlin shell finite elements for discretization in order to construct an optimization approach that is numerically efficient & also restrict the length of the product to ensure that it can be manufactured as shown in figure 2.

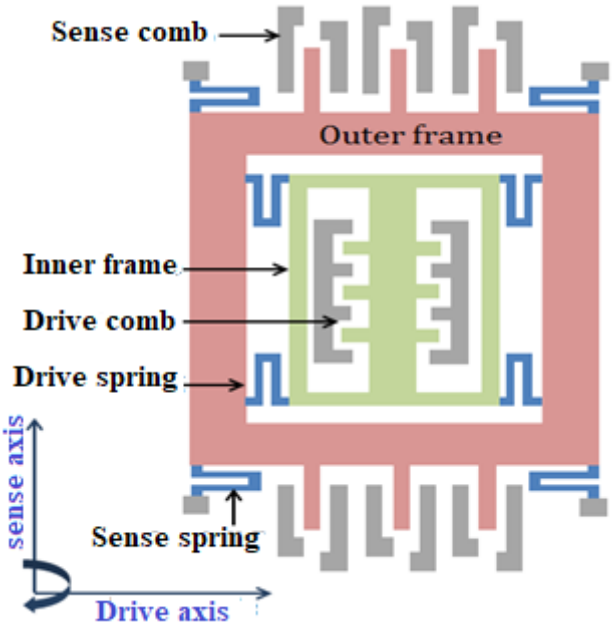

Figure 2 MEMS resonator designs for gyroscope use

Low-power, low-cost RF devices for use in high-frequency applications have been developed because to advancements in MEMS technology. As the need for low-cost, high-performance, and small wireless communication systems grows, so does the number of new radio frequency devices be developed. A low return loss, high capacitance ratio, and low power consumption ratio are only a few of the shortcomings of conventional semiconductor devices compared to RF MEMS switches. For frequencies from microwaves to millimeter waves, RF MEMS switches with PIN diodes outperform FETs hands-down.

Capacitive Shunt Switch Design and Simulation in FEM Tool: Capacitive shunted switches, which are fixed- structures in the FEM Tools, are the subject of this paper, which details their designs and simulations using the FEM Tools. An improvement in switching performance is achieved by adding meanders, perforations, and a moveable beam to the current configuration; these structural changes also consist the inclusion of the step-down beam. A bridge-like gap between the fixed and moveable beams in all but the step-down structures fixed and moveable beams are parallel.

Advanced innovation is aimed at sending tiny satellites into orbit weighing less than one kg. Micro electro mechanical systems (MEMS) may be used in a wide range of applications, from military systems to consumer electronics to automobiles to RADAR and communication systems. A growing interest in RF devices like switches and switched capacitors, resonator inductors and variable inductors has spurred the creation of a slew of new RF devices. It is possible to utilize RF MEMS switches in radar and satellite communication due to their cheap cost, low power consumption, and high reliability. Equipment such as these switches are critical to the operation of satellite uplink and downlink networks. This makes them excellent for networks and antenna systems since they are more reliable than standard switches (PIN diodes, FETs and transistors) in microwave applications.

The RF MEMS switches are constructed using a combination of metal, semiconductors, and insulators in the proposed configuration. MEMS switches may be built using a wide variety of materials including substrates (Si, Ge, GaAs and quartz), insulators (SiO2 and Si3N4) and conductors (Cu, Au, Al) for transmission lines in the micrometer-thick range. Nanoscale range metal membranes (Ex.: Al, Au, Cu) are referred to as actuating beams and electrodes, as shown in Figure 3.

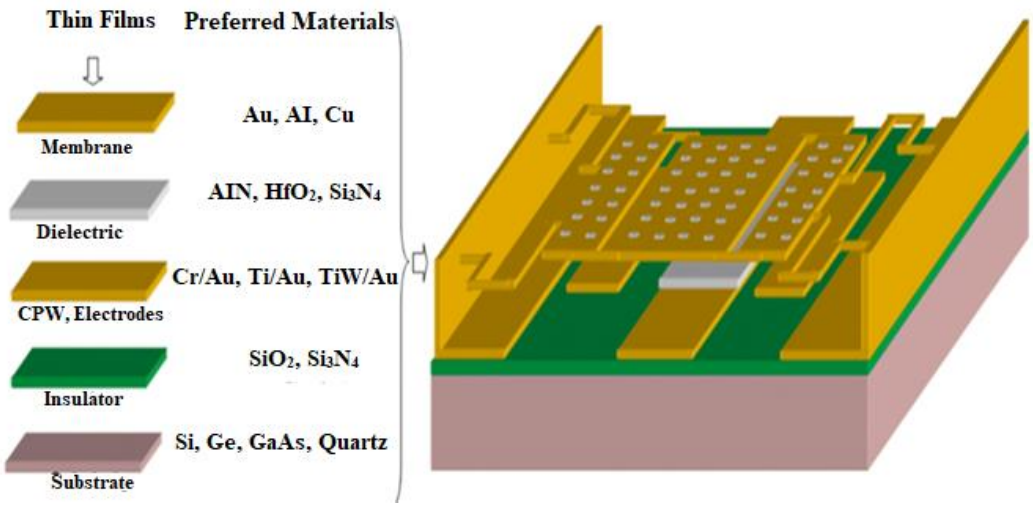

Figure 3 RF MEMS switch layer-by-layer schematic diagram

Reduced voltage is needed to activate the suggested switch since thin membranes with holes were used. The holes in the switch will aid in the ease of electrostatic actuation and enlarge the segregation of the circuit

3. Proposed RF MEMS switch methodology

In this section, describes proposed RF MEMS switch performance followed by the activation of micro-level membrane structures is a primary component of MEMS technology-based devices. Electrostatic actuation is preferred since it is easier to implement and more effective. The switch's performance and properties may be studied using the spring constant as a major parameter. The proposed design has been crossover the miss-functionalities of uncertain RF-MEMS switching activity.

3.1. Proposed Arrangement for Uniform Meander RF MEMS Switch

In order to study the RF MEMS switch's electrical and mechanical characteristics, the FEM, or Finite Element Method, is used in COMSOL Multi-Physics software. A flaw in the beam's movement is generated by electromechanical forces in order to activate the switch. Therefore, a 0.8 m gap between the dielectric and moving beam is recommended, and HfO2 is used as the dielectric material. If you have 2.5 V as the pull-in voltage, a switch with 8.27 *10-3 and 0.01 in the negative direction of z-component displacement is possible.

RF MEMS (Radio Frequency Micro Electro Mechanical Systems) is a promising and relatively new technique for the development of switching devices. As the word implies, it's a cross-disciplinary

one. The gadget has a size range of one micrometer to one hundred micrometers (m). MEMS devices integrate and enhance electro-mechanical and semiconductor switches, such as PIN diodes and FETs, as well as waveguide and coaxial switches. The micron-sized components provide for several benefits, such as lower power consumption, lower costs, linearity, lower operating voltages, higher isolation, higher reliability, lower insertion loss, and the possibility to produce vast arrays of the components in question. Antennas and space systems are just a few of the numerous applications that may make use of this amazing technology due to its wide range of useful properties. These switches are developed primarily for microwave applications such as mobile phones and short-range communications such as Bluetooth and WLAN, automotive sectors.

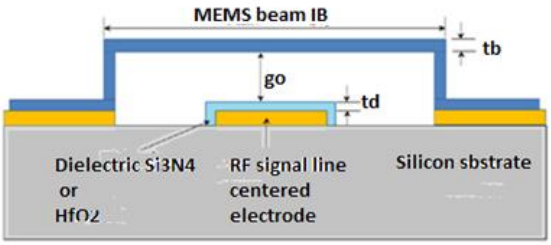

Figure 4 Representation of proposed uniform meander RF MEMS switch

Shunt RF MEMS Switches with high Con Coff ratios and extensive comparisons of three meander beams and one meander beam RF MEMS switches are provided in this study. 5–40 GHz is the frequency range that RF MEMS Switches are meant to operate in shown in figure 4.

3.2. Dimensions of uniform meander switch

In this section through Tables 1 demonstrate how four-node linear quadrilateral Mindlin shell finite elements moved in and out of a plane in this study's planar MEMS geometries. Choosing this kind of component was made because it strikes a reasonable balance between accuracy and processing costs. Increasing the accuracy of linear brick hexagonal elements would necessitate considering at least four such elements, and this would result in computational costs that are too high for our optimization needs and could easily lead to memory saturation issues for the 16 GB RAM that we are considering.

Table 1 Dimensions of the uniform meander switching device

Indicators	**Elements**	**Measurements**
G/S/G	Coplanar waveguide	$56\mu m/95.00\ \mu m/56.00\ \mu m$
H	Height of the substrate	$400.00\ \mu m$
W	Membrane bridge beam width	$186.00\ \mu m$
L	Air gap	$558.00\mu m$
go	Air gap Dielectric thickness	$3.00\ \mu m$
Td	Thickness of Dielectric	$00.2\ \mu m$
As	Square holes	$(06*06)\mu m$
A	Actuation area	$186.00\ \mu m * 270.00\mu m$

The below table 2 clearly explains uniform meander dimensions, here Length, breadth and thickness are improved compared to K1 as well K2 indications.

Table 2 Uniform meander dimensions

Indicators	Length	Breadth	Thickness
K1	48 $\boldsymbol{\mu m}$	5.**00** $\boldsymbol{\mu m}$	01.2 $\boldsymbol{\mu m}$
K2	55 $\boldsymbol{\mu m}$	05 $\boldsymbol{\mu m}$	01.2 $\boldsymbol{\mu m}$

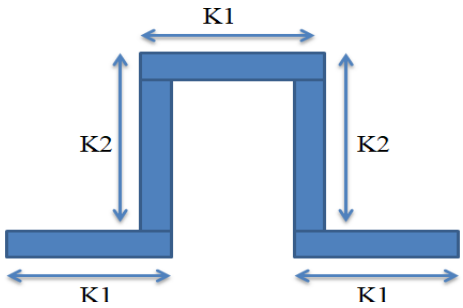

Figure 5 Representation position of Uniform Meander

The above figure 5 is suitable for future RF MEMS switch design, the position as well as representation is providing information about MEMS size and area consumption.

4. Hypothetical considerations of uniform meandering switch

4.1. Spring constant Impact

A trade-off is being generated among spring constant and pull-in voltage (shown in figure 5). With minimal spring constant, the pull-in voltage obtained is minimum [17]. Mathematically, the spring constant is stated as

$$k = \frac{Ewt^3}{L^3} = 3.588N/m \qquad (1)$$

Where K symbolized Spring Constant then width is W, thickness is t, and L is length correspondingly.

4.2. Pull in voltage Impact

Expressed in a quantity of needed voltage value for the purpose of beam towards pulling down as well as associate with the signal dielectric. And is formulated as, [18]

$$V_p = \sqrt{\frac{8Kg^3}{27\ \epsilon_0\ A}}\ \ Volts = 8.06\ Volts \qquad (2)$$

Parting of electrode as of beam is indicated by 'g', whereas, free space permittivity is denoted with 'ε_0', and actuation area is 'A'.

4.3. Impact with ON state capacitance (C_{ON})

With the measured switch capacitance attained in the provision of displacement induced with the beam, attained signal dielectric property, expressed by Upstate Capacitance C_{ON}. Mathematically evaluated with respect to,

$$C_{ON} = \sqrt{\frac{\epsilon_0\ \epsilon_r\ xy}{g + \frac{t_d}{\epsilon_r}}}\ \ Farad = \ 103\ \ f\ Farads \qquad (3)$$

Width of the beam is given with the parameter x, Beam length denoted with y, Gap obtained at beam to dielectric path is given as g, whereas, t_d holds the thickness of dielectric, ε_r denotes beam material relative permittivity.

4.4. OFF state Capacitance (C_{OFF}) Effect

Switch associating the capacitor under the contact of beam towards the signal dielectric, for instance air gap does not exist is termed to be downstate capacitance.

Mathematical formulation is given as,

$$C_{OFF} = \sqrt{\frac{\epsilon_0 \epsilon_r\ xy}{t_d}}\ Farad = 7.03\ pFarads \qquad (4)$$

Beam width is given with the parameter x, Beam length denoted with y, Gap obtained at beam to dielectric path is given as g, whereas, t_d holds dielectric thickness, ε_r denotes beam material relative permittivity.

4.5. Impact of Capacitance ratio (C_{ratio})

Given as transition of capacitance from OFF to the ON states.

$$C_{ratio} = \frac{C_{OFF}}{C_{ON}} = 68.25 \qquad (5)$$

4.6. Switching time analysis Impact

Period necessities to initiate the transition amount inherently within the ON state shifted among the field of OFF-State & from OFF-State to ON-State determines the period of switching [19] along with formulating the equation as follows,

$$T_s = \frac{3.67\ V_p}{V_s \omega_0} Seconds \qquad (6)$$

V_P signifies Pull-in voltage, V_s symbolizes Voltage supply, ω_0 holds frequency resonance. Consequently, switching time corresponds towards 00.14msec.

4.7. Impact of Quality Factor

Depends upon damping coefficient, spring constant, and resonant frequency. Applicable for diminishing the sustenance under the selection of actuation through the electrode among various dimensions along with fixed beam value, as reason to minimize the te air gap among actuation electrode [20]. Further, the measured mathematical formulation is as follows,

$$b = \frac{3}{2\pi} \frac{\mu A^2}{g^3} = 0.033 \times 10^{-3} \qquad (7)$$

'μ' symbolizes the Viscosity of air, 'A' stands for Area as well as parting of electrode as of beam is given as 'g'. Mathematically 'Q' is given as

$$Q = \frac{K}{2\pi f_0 b} \qquad (8)$$

At any instant quality factor must be chosen among the range of 0.5 and 2. Enhancement of switching activity is accomplished with the anticipated switching methodology attaining accurate Q factor about 0.550.

4.8. Selection of *Substrate Material*

Various feasible appropriate materials required for substrate in addition to the individual graphs that has been plotted among the relation of Poisson's distribution ratio towards young's modulus as depicted in figure 6 for necessity of silicon material as substrate material as enhanced.

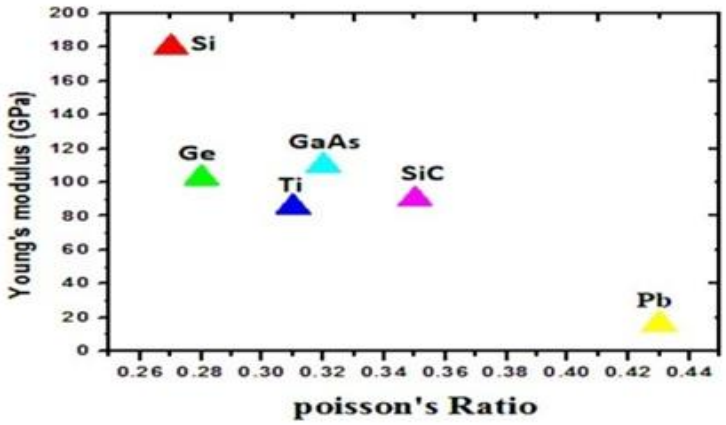

Figure 6 Switch selection considering Substrate material

Greater range of stiffness factor is attained with support of Poisson's ratio and Young's modulus. Overall performance enhancement of switch is done through impedance mapping within the system depending on form of dielectric constant with substrate material [21]. Moreover, preferred element is Silicon, since it is suitable substrate material due to its maximum resistivity, phase velocity, combined with cost-effective nature [22-23]. Greater value of dielectric constant for instance 11.9 extends towards minimal signal loss. Furthermore, the crucial aspect is about the CPW dimensions showing principal responsibility in RF signal transmission as depicted in figure 6 [24].

4.9. Selection of *Dielectric Material*

Numerous materials have been chosen for evaluating the ideal or standard materials for the purpose of signal dielectric as shown in table 3. It will be processed depending on dielectric constants at maximum and medium range.

Table 3 Different Dielectric Material Properties

Type of material	$\boldsymbol{\varepsilon_r}$	***Resistivity (ρ)***	$^{\mathbf{1}}/_{\boldsymbol{\varepsilon_r}}$	$\mathbf{log}(\boldsymbol{\rho})$
SiO_2	003.9	01.00E+14.00	00.25641	14
$Si3N_4$	007.5	01.00E+14.00	00.133333	14
$Al2O_3$	009.8	01.00E+14.00	00.102041	14
A1N	008.5	01.00E+14.00	00.117647	14
HfO_2	25.00	01.00E+14.00	00.04	014

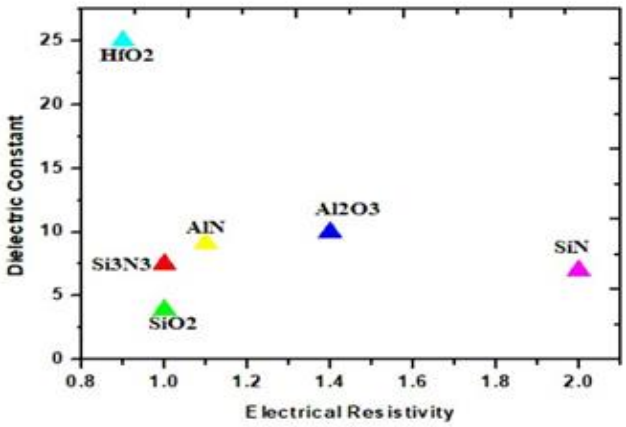

Figure 7 Switch selection considering Dielectric material

These Dielectric qualities increase design, processing, quality, and control. Complex permittivity (r*) explains a material's behavior in an electromagnetic field. Dielectronic substance stores energy when an external electric field is applied. The above figure 7 is clearly explains about deep switching analysis of designed Di-electric material, here resistivity as well as dielectric properties are verified with Ansoft High frequency structure simulator (HFSS) tool. [25].

4.10. Beam Material Selection

In this section a beam material parameter has been analyzing, the beam materials like Gold, aluminum, platinum and si3N4 are giving less improvement in E(Gpa) but compared following proposed Sio2 based materials can be most suitable in operations shown in table 4.

Table 4 Properties of different beam materials

Material type	E (Gpa)	rho	$\sqrt{E}$	$\sqrt{E/\rho}$
Gold	79.00	019.3	8,88819.00	02.02318
Aluminum	70.00	02.7	8.83666.00	05.09175
Platinum	168.00	021.45	12.96148.00	02.7987
Si3N4	385.00	03.1	019.62142	011.14422
Ni	200.00	08.902	014.14214	04.73992
Si	196.00	02.3	14.00	09.23133
SiO2	73.00	02.27	08.544	05.67085

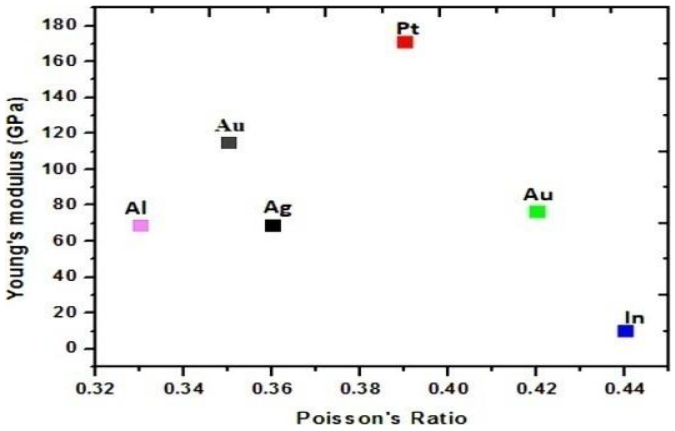

Figure 8 Switch Material selection for Beam switch

Intended for choosing to beam relevant assortment numerous appropriate substances are usually analyzed in addition to correct or modify the graphical representations among several indices in relation to young's module and Poisons ratio. Depending upon element chosen, the performance analysis has been demonstrated which is depicted in figure 8, for the little Poisson's ratio coupled with medium young's modulus. Among several materials, Aluminum is found as suitable one. Whereas elements such as Au (Gold) are highly expensive when compared to Al (Aluminum), hence, it is evident to choose aluminum for beam substance since Al is desired as the suitable element for beam as explained in table 5.

Table 5 Selection of proposed RF MEMS switch material

Selection	Material Type
Substrate	Si
CPW Guide	Al
Dielectric layer	HfO_2
Anchors	Al
Fixed beam	Al

The above table 5 is explaining clear picture of material type Si, Al, Hfo2, AI and AI (anchors), in this proposed material attains more improvement.

5. Outcomes and Discussions

In this section provides a brief note on comparison of the improved layouts' performance with that of complete model simulations has shown their efficacy. With these data we can see how well-performing resonators perform when using lower order models instead of full models to optimize the

resonance frequency. Fine-tuning an existing design is simple when the final application asks for 50 additional optimization stages, each of which only needs full models for out-of-plane dynamics in the final phase.

At long last, our study opens the door to the optimizations of many MEMS resonant structures, such accelerometers, microphones, micro mirrors, and curved shell resonators. The technique may be used to accounting for mechanical non - linearities and coupled physics, such as electro-mechanical and acoustic-mechanical interactions.

5.1. *Electro-mechanical Analysis for uniform meander switch*

Case i) Beam materials interchanging

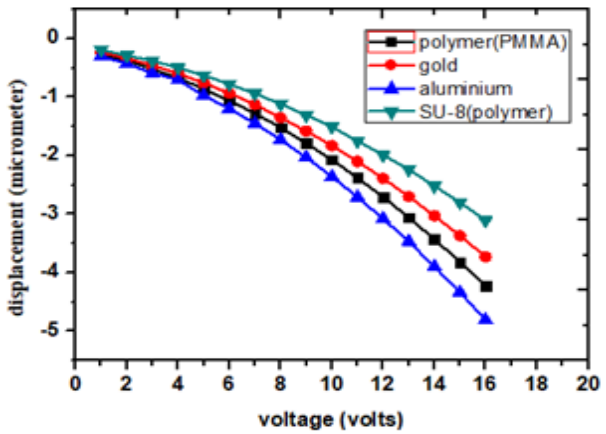

Figure 9 Change in voltage and displacement under various materials

Piezoelectric, thermal, and electromagnetic controllers are used in RF MEMS switches. Thermo and mechanical actuation technologies are less favored over electrical actuation methods due to manufacturing complexity, even though they need less pull in voltage to deflect a beam. However, with electrostatic actuator, this study must contend with the difficulties of obtaining a large draw in voltage while maintaining a low switching frequency shown in figure 9

Case ii) Gaps interchanging

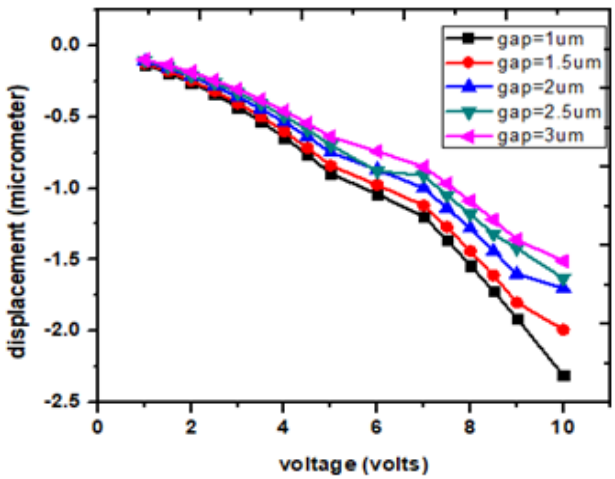

Figure 10 Distinctive gaps for voltage and displacement

The upstage capacitive determines absorption and return loss, while the downward state resistance determines isolating. The capacitive ratio reflects the effectiveness of the RFMEMS switching. Using a high-K piezoelectric medium enhances the capacitive ratio of the switch, resulting in improved switch functionality via the S-parameter. With a gap of 0.8 mm between the electrostatic beam and the dissipation factor, Si3N4 with a dielectric permittivity of 7.6 gives C ratios of 8.69 and

11.13 for 0.8 and 0.6 lm of beam width, respectively, whilst HfO2 with a dielectric of 14 gives C-ratios of 14.93 and 19.66 for 0.8 and 0.6 lm of beam surface area, respectively shown in figure 10
Case iii) Distinctive dielectric materials interchange.

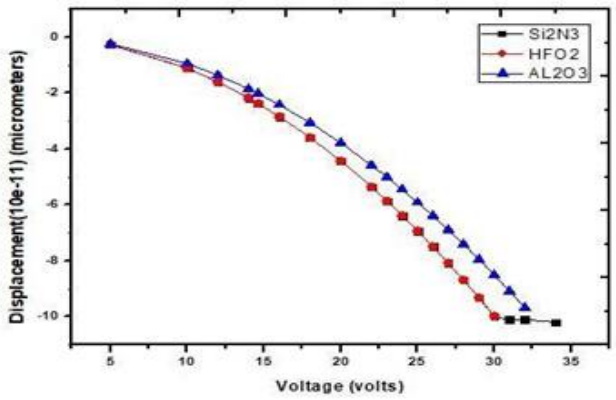

Figure 11 Variation with dielectric materials with respect to Voltage and displacement

Circuits with various curved meanders and holes have been devised, resulting in a lower constant, lower pull-in voltage, high isolation loss, fast switching velocity, and reduced insertion loss. While comparing rectangle perforated to square and cylindrical shaped perforation, the modeled findings show that rectangle incisions provide superior outcomes shown in figure 11

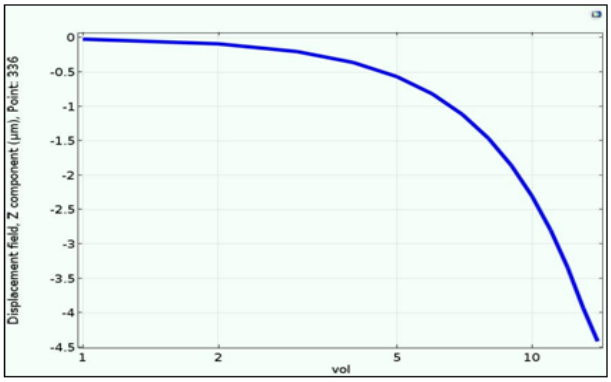

Figure 12 Curve resulting relation among Voltage and displacement

From each construction, a comparison has been done for the meandering, addition, and triple large rectangular meanders, as well as rectangular perforation. The up-state capacitance for HfO2 is 4.06fF and for Si3N4 is 3.80fF when the spacing in between insulation and the moveable beam is 0.8 m. HfO2 and Si3N4 have downstate capacitances of 49fF and 26.9fF, accordingly shown in figure 12

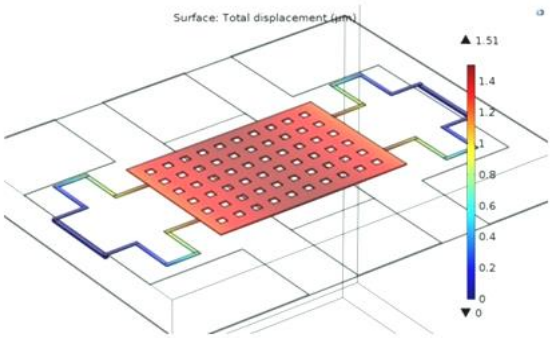

Figure 13 Total displacement obtained on behalf of pll-in Voltage over FEM tools

The above figure 13 is clearly explains about displacement ad pull voltage analysis over FEM, this design is most suitable for future RF-MEMS switch applications.

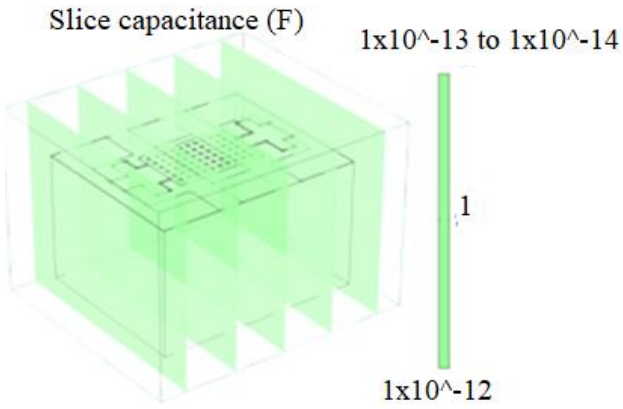

Figure 14 Capacitance state under the condition of Simulated ON

Investigators can get more isolation at higher frequencies by utilizing a larger bridge width and a bigger downstate capacitance. Return loss approaches 0 dB in the activated state at higher frequencies, and it may be further enhanced by altering the breadth. S parameters are simulated using HFSS software for uniform single, double, triple meanders, and non-uniform single meander structures by changing the dielectric material to HfO2 and Si3N4 shown in figure 14.

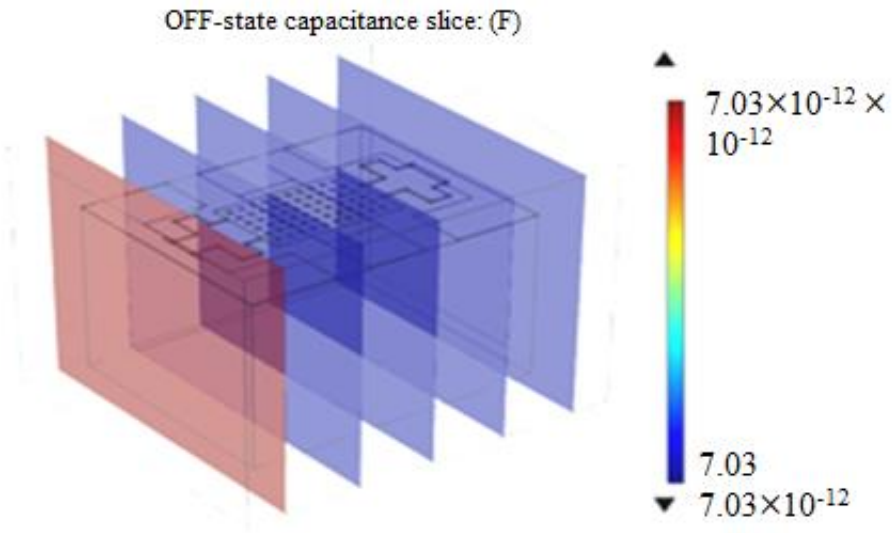

Figure 15 State capacitance under the condition of Simulation OFF

The above figure 15 is clearly explains about state capacitance as well as simulated OFF modeling mechanism, in this off-capacitance state is denoted with F as well as 7.03x10^-12 F is varied through HFSS tool. $7.03\times10^{-12}\times10^{-12}$

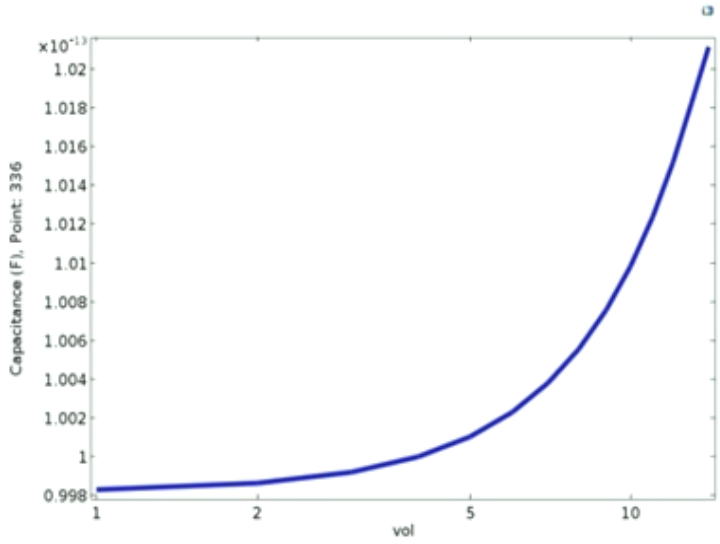

Figure 16 Uniform meander switch C-V curve

It is constructed and evaluated capacitance shunt MEMS switches with various numbers of meanders. In general, RF MEMS switches are widely used in networking, and numerous switches have been designed with diverse architectures focusing mostly on pull in voltage shown in figure 16.

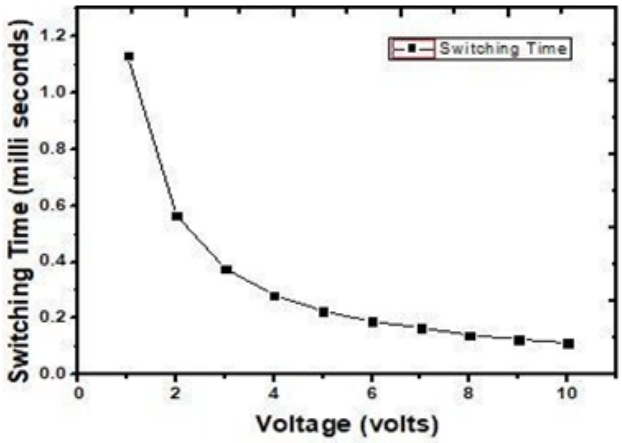

Figure 17 Uniform meander switching time

"Switching time" refers to the amount of time it takes a switch to go from being active to being inactive, and vice versa. Figure 17 shows the proposed uniform meander switching time in detail. The plot of voltage against switching time shows that the switching time is much improved over prior models and non-uniform meander switching time.

5.2. Stress analysis

Under various elements, best chosen for beam purpose is aluminum which has the property to demonstrate a stress analysis approximately around 1.78E-5Pa along with enforced valued at 1.9606E -6N.

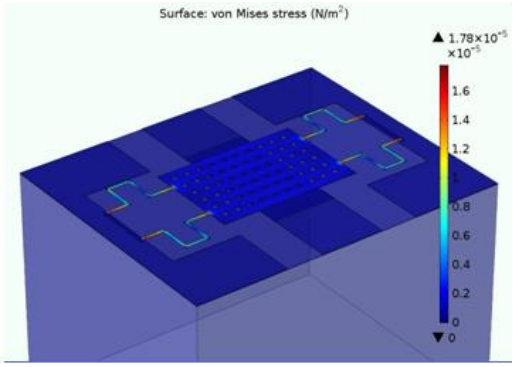

Figure 18 Analysis of Stress distribution

The figure 18 is clearly explains about analysis of stress distribution modeling compared to earlier models proposed stress distribution is giving more improvement.

5.3. Electromagnetic Analysis for Uniform Meander Switch

On and off-state performance are improved with the new MEMS switch. A good return loss and insertion loss may be achieved in both the UP and DOWN (OFF) states, respectively. With low losses and high isolation values, this suggested switch may be used across a wide range of frequencies from zero to 38 gigahertz. The suggested device is best suited for radar and satellite communications in this frequency band.

Return Loss: This has been taken into consideration due to misalliance with the impedance amid the circuits as depicted in Figure 19.

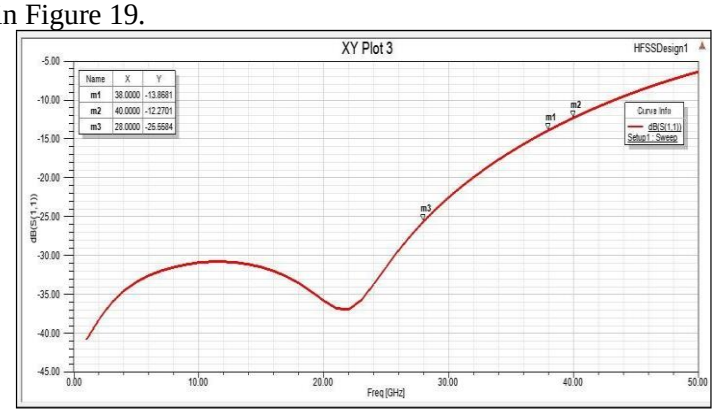

Figure19 Return loss for Uniform meander switch

Insertion loss: In comparison to supplementary selected frequency, tends to critical condition in testing or evaluating the insertion loss. It is cost-burdened with high range power frequencies. Therefore, there will be provision for electromechanical switches under shortest feasible loss as depicted in Figure 20.

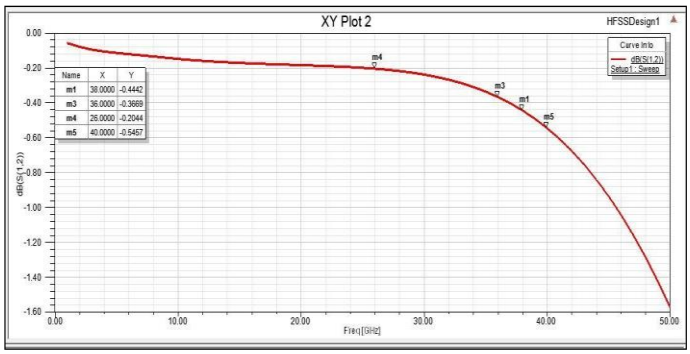

Figure 20 Insertion loss for Uniform meander switch

***Isolation loss*:** Defined as attenuation level obtained through undesirable detected signal by the interfacing degree of freedom. Moreover, it is essential for superior range of frequencies.

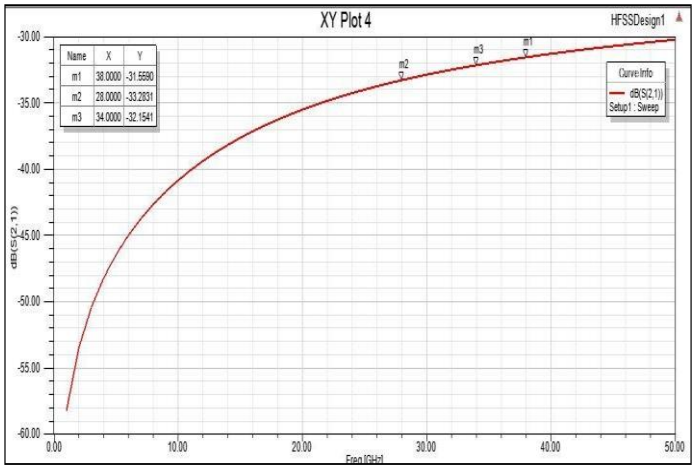

Figure 21 Isolation loss in Uniform meander switch

The figure 21 is clearly explains about uniform isolation loss with respected to meander switch, in this frequency vs gain dB parameters has been analyzed compared to existed models proposed material with RF MEMS switch giving improvement in terms of Gain and frequency.

6. Conclusion

The design of RF-MEMS design has been improved for artificial intelligence applications. Radio detection and ranging has been employed through RF MEMS technology. This study focuses on optimization model, which is functioned at 35GHz. However, dimensions of the uncertain switches are altered with respect to the previous measurements as integration through optimization methodology. Further modifications in the dimensions of proposed switch are done through the optimization methodology. Enhancement of functional behavior is attained with the optimization by the count under isolation range having -31.56dB within the 8.06V pull-in voltage with the spring constant quantity of 3.588N/m. Making use of the COMSOL software, MEMS switches are designed and simulated the programme & also the entire analysis of electromechanical assessment is performed intended in evaluating capacitance value for the case of Downstate then Upstate, range of pull in voltage combined with stress assessment. In addition, proposed RF MEMS switch will efficiently incorporate equivalent relation to switching portion contained by the antenna patches towards the reconfiguration attainment on superior frequency range about 38GHz. Consequently, the switch will be most excellent capable in support of upcoming communications applications that include 5G technology.

References

[1] Iannacci, J. (2020). RF-MEMS for 5G applications: a reconfigurable 8-bit power attenuator working up to 110 GHz. Part 1: design concept, technology and working principles. Microsystem technologies, 26(3), 675-687.

[2] Muldavin, J. B., & Rebeiz, G. M. (2000). High-isolation CPW MEMS shunt switches. 1. Modeling. IEEE transactions on microwave theory and techniques, 48(6), 1045-1052.

[3] Shen, Q., & Barker, N. S. (2005). A reconfigurable RF MEMS based double slug impedance tuner. In 2005 European Microwave Conference (Vol. 1, pp. 4-pp). IEEE.

[4] Pacheco, S. P., Katehi, L. P., & Nguyen, C. C. (2000). Design of low actuation voltage RF MEMS switch. In 2000 IEEE MTT-S International Microwave Symposium Digest (Cat. No. 00CH37017) (Vol. 1, pp. 165-168). IEEE.

[5] Chu, C., Liao, X., & Yan, H. (2017). Ka-band RF MEMS capacitive switch with low loss,

high isolation, long-term reliability and high-power handling based on GaAs MMIC technology. IET Microwaves, Antennas & Propagation, 11(6), 942-948.

[6] Katehi, L. P., Harvey, J. F., & Brown, E. (2002). MEMS and Si micromachined circuits for high-frequency applications. IEEE Transactions on Microwave Theory and Techniques, 50(3), 858-866.

[7] Roh, W., Seol, J. Y., Park, J., Lee, B., Lee, J., Kim, Y., & Aryanfar, F. (2014). Millimeter-wave beamforming as an enabling technology for 5G cellular communications: Theoretical feasibility and prototype results. IEEE communications magazine, 52(2), 106-113.

[8] Sattler, Robert, Florian Plötz, Gernot Fattinger, and Gerhard Wachutka. "Modeling of an electrostatic torsional actuator: demonstrated with an RF MEMS switch." Sensors and Actuators A: Physical 97 (2002): 337-346.

[9] Rahim, M. K. A., Hamid, M. R., Samsuri, N. A., Murad, N. A., Yusoff, M. F. M., & Majid, H. A. (2016, October). Frequency reconfigurable antenna for future wireless communication system. In 2016 46th European Microwave Conference (EuMC) (pp. 965-970). IEEE.

[10] Hong, W., Baek, K. H., & Ko, S. (2017). Millimeter-wave 5G antennas for smartphones: Overview and experimental demonstration. IEEE Transactions on Antennas and Propagation, 65(12), 6250-6261.

[11] Mahmoud, K. R., & Montaser, A. M. (2018). Design of dual-band circularly polarised array antenna package for 5G mobile terminals with beam-steering capabilities. IET Microwaves, Antennas & Propagation, 12(1), 29-39.

[12] Demirel, K., Yazgan, E., Demir, Ş., & Akın, T. (2015). A new temperature-tolerant RF MEMS switch structure design and fabrication for Ka-Band applications. Journal of Microelectromechanical Systems, 25(1), 60-68.

[13] Molaei, S., & Ganji, B. A. (2017). Design and simulation of a novel RF MEMS shunt capacitive switch with low actuation voltage and high isolation. Microsystem Technologies, 23(6), 1907-1912.

[14] Kumar, P. A., Sravani, K. G., Sailaja, B. V. S., Vineetha, K. V., Guha, K., & Rao, K. S. (2018). Performance analysis of series: shunt configuration-based RF MEMS switch for satellite communication applications. Microsystem Technologies, 24(12), 4909-4920.

[15] Pertin, O. (2018). Pull-in-voltage and RF analysis of MEMS based high performance capacitive shunt switch. Microelectronics Journal, 77, 5-15.

[16] Ravirala, A. K., Bethapudi, L. K., Kommareddy, J., Thommandru, B. S., Jasti, S., Gorantla, P. R., ... & Karumuri, S. R. (2018). Design and performance analysis of uniform meander structured RF MEMS capacitive shunt switch along with perforations. Microsystem Technologies, 24(2), 901-908.

[17] Sateesh, J., Girija Sravani, K., Akshay Kumar, R., Guha, K., & Srinivasa Rao, K. (2018). Design and flow analysis of MEMS based piezo-electric micro pump. Microsystem Technologies, 24(3), 1609-1614.

[18] Venkateswarlu, M., Prasad, M. V. V. K. S., Swapna, K., Mahamuda, S., Rao, A. S., Babu, A. M., & Haranath, D. (2014). Pr3+ doped lead tungsten tellurite glasses for visible red lasers. Ceramics International, 40(4), 6261-6269.

[19] Mohan, C. L., Kavya, K. C., & Kotamraju, S. K. (2021). Design, and Analysis of Capacitive Shunt RF MEMS Switch for Reconfigurable Antenna. Transactions on Electrical and Electronic Materials, 22(1), 57-66.

[20] Morzelona, R. (2021). Human Visual System Quality Assessment in The Images Using the IQA Model Integrated with Automated Machine Learning Model. Machine Learning Applications in Engineering Education and Management, 1(1), 13–18.

[21] Dhabliya, D. (2021). Feature Selection Intrusion Detection System for The Attack Classification with Data Summarization. Machine Learning Applications in Engineering Education and Management, 1(1), 20–25.

[22] Rao, K. S., Kumar, P. A., Guha, K., Sailaja, B. V. S., Vineetha, K. V., Baishnab, K. L., & Sravani, K. G. (2021). Design and simulation of fixed–fixed flexure type RF MEMS switch for reconfigurable antenna. Microsystem Technologies, 27(2), 455-462.

[23] Lakshmi Narayana, T., Girija Sravani, K., & Srinivasa Rao, K. (2017). Design and analysis of CPW based shunt capacitive RF MEMS switch. Cogent Engineering, 4(1), 1363356.

[24] Gandhi, S. G., Govardhani, I., Kotamraju, S. K., Kavya, K., Prathyusha, D., Rao, K. S., & Sravani, K. G. (2020). Improve the performance of a novel capacitive shunt RF MEMS switch by beam and dielectric materials. Transactions on Electrical and Electronic Materials, 21(1), 83-90.

[25] Mohan, C. L. (2021). Design and Analysis of a Non-Uniform Meander RF MEMS Switch. Information Technology in Industry, 9(2), 756-767.

[26] Padmini, G. R., Rajesh, O., Raghu, K., Sree, N. M., & Apurva, C. (2021, March). Design and analysis of 8-bit ripple Carry Adder using nine transistor full Adder. In 2021 7th International Conference on Advanced Computing and Communication Systems (ICACCS) (Vol. 1, pp. 1982-1987). IEEE.

[27] Prof. Nikhil Surkar. (2015). Design and Analysis of Optimized Fin-FETs. International Journal of New Practices in Management and Engineering, 4(04), 01 - 06.

[28] Qureshi, D. I. ., & Patil, M. S. S. . (2022). Secure Sensor Node-Based Fusion by Authentication Protocol Using Internet of Things and Rfid. Research Journal of Computer Systems and Engineering, 3(1), 48–55.

[29] Ramaiah, V. S., Singh, B., Raju, A. R., Reddy, G. N., Saikumar, K., & Ratnayake, D. (2021, March). Teaching and learning based 5G cognitive radio application for future application. In 2021 International Conference on Computational Intelligence and Knowledge Economy (ICCIKE) (pp. 31-36). IEEE.